



# CHORUS

This is the accepted manuscript made available via CHORUS. The article has been published as:

## How order melts after quantum quenches

Mario Collura and Fabian H. L. Essler

Phys. Rev. B **101**, 041110 — Published 23 January 2020

DOI: [10.1103/PhysRevB.101.041110](https://doi.org/10.1103/PhysRevB.101.041110)

# How order melts after quantum quenches

Mario Collura<sup>1,2</sup> and Fabian H.L. Essler<sup>3</sup>

<sup>1</sup>*Theoretische Physik, Universität des Saarlandes, D-66123 Saarbrücken, Germany.*

<sup>2</sup>*Dipartimento di Fisica e Astronomia “G. Galilei”, Università di Padova, I-35131 Padova, Italy*

<sup>3</sup>*Rudolf Peierls Centre for Theoretical Physics, Oxford University, Oxford, OX1 3PU, United Kingdom*

Injecting a sufficiently large energy density into an isolated many-particle system prepared in a state with long-range order will lead to the melting of the order over time. Detailed information about this process can be derived from the quantum mechanical probability distribution of the order parameter. We study this process for the paradigmatic case of the spin-1/2 Heisenberg XXZ chain. We determine the full quantum mechanical distribution function of the staggered subsystem magnetization as a function of time after a quantum quench from the classical Néel state. We establish the existence of an interesting regime at intermediate times that is characterized by a very broad probability distribution. Based on our findings we propose a simple general physical picture of how long-range order melts.

*Introduction.* — A fundamental objective of quantum theory is to determine probability distribution functions of observables in given quantum states. In few-particle systems the time evolution of such probability distributions provides a lot of useful information beyond what is contained in the corresponding expectation values. Recent advances in cold-atom experiments have made possible not only the study of non-equilibrium time evolution of (almost) isolated many-particle systems [1–13], but given access to the full quantum mechanical probability distributions of certain observables [14–18]. This provides an opportunity to gain new insights about the coherent dynamics of many-particle quantum systems. One intriguing question one may ask is how order melts, or forms, when an isolated many-particle system is driven across a phase transition. Related questions have been studied in solids, but there one essentially deals with open quantum systems and has access to very different observables, see e.g. [19–21]. The basic setup we have in mind is as follows. Let us consider a system of quantum spins with Hamiltonian  $H$  that is initially prepared in a state with density matrix  $\rho(0)$ . In this state there is long-range order characterized by an order parameter  $\mathcal{O} = \sum_{j=1}^L \mathcal{O}_j$ , where  $j$  runs over the sites of the lattice and  $\mathcal{O}_j$  is a local operator. We are interested in the probability distribution function (PDF)  $P_A$  of the order parameter  $\mathcal{O}_A$  in a contiguous subsystem of linear size  $|A|$

$$P_A(m, t) = \text{Tr}[\rho(t)\delta(\mathcal{O}_A - m)]. \quad (1)$$

Here  $\rho(t)$  is the density matrix of the system at time  $t$  and  $P_A(m, t)$  is the probability that the subsystem order parameter  $\mathcal{O}_A$  takes the value  $m$  in the state  $\rho(t)$ . We are interested in cases where the system is initially well ordered at all length scales and  $P_A(m, t)$  is therefore narrowly peaked around the average  $\mathcal{O}_A$ . Under time evolution the order melts and at late times and large subsystem sizes  $P_A(m, t)$  is believed to approach a Gaussian distribution centred around zero [22–28]. The question of interest is how  $P_A(m, t)$  evolves as a function of time

and subsystem size  $|A|$ . Varying the latter provides information about how well the system is ordered at length scale  $|A|$ .

We find that when the initially ordered system is quenched well into the unbroken symmetry phase of the Hamiltonian, the (local) order quickly disappears and the PDF acquires a simple Gaussian shape. In contrast, when the quantum quench is to an energy density where Hamiltonian eigenstates retain short-range order[29], the PDF exhibits a complex structure both at finite times and in the stationary state. In the following we focus on the example of the spin-1/2 Heisenberg XXZ chain, but note that the picture we put forward is general and has a wide range of applicability.

*Model and Setup.* — We investigate the time evolution of antiferromagnetic (short-ranged) order after a quantum quench in the spin-1/2 XXZ chain

$$H_\Delta = \sum_j S_j^x S_{j+1}^x + S_j^y S_{j+1}^y + \Delta S_j^z S_{j+1}^z. \quad (2)$$

Here  $S_j^\alpha$  are spin-1/2 operators acting on the site  $j$  and we restrict our analysis to the range  $\Delta > 0$ . The phase diagram of (2) is well established: at  $T = 0$  there is a BKT phase transition at  $\Delta = 1$  that separates a quantum critical phase at  $\Delta < 1$  and an antiferromagnetically ordered phase at  $\Delta > 1$ . At any finite temperature the antiferromagnetic order melts. The Hamiltonian (2) is invariant under rotations by an arbitrary angle around the z-axis, translations by one site, and rotations around the x-axis by 180 degrees. In the thermodynamic limit at  $\Delta > 1$  and zero temperature the last symmetry gets broken spontaneously and one of the two degenerate ground states  $|\text{GS}_\Delta^\pm\rangle$ , characterized by equal but opposite expectation values of the staggered magnetization per site, gets selected. In the Ising limit  $\Delta \rightarrow \infty$  the ground states become the classical Néel states, i.e.  $|\text{GS}_\infty^+\rangle = |\cdots \uparrow\downarrow\uparrow\downarrow \cdots\rangle$  and  $|\text{GS}_\infty^-\rangle = |\cdots \downarrow\uparrow\downarrow\uparrow \cdots\rangle$ . In order to investigate the melting of antiferromagnetic order we consider the following quantum quench protocol: (i) we prepare the system in the classical Néel state

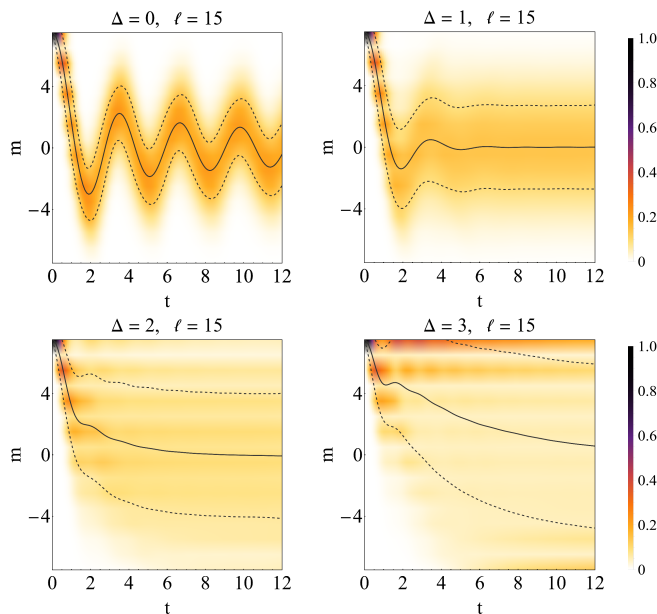


FIG. 1. Density plot of  $\tilde{P}_\ell(m, t)$  with  $m \in [-\ell/2, \ell/2]$  and  $t \in [0, 12]$  for a subsystem size  $\ell = 15$ , after a quench from the Néel state  $|\text{GS}_\infty^+\rangle$  to  $\Delta = 0, 1, 2, 3$ . The full line represents the expectation value  $\bar{m}(t)$ , the dashed lines are the standard deviation from the average, namely  $\bar{m}(t) \pm \sigma(t)$ .

$|\Phi_0\rangle = |\text{GS}_\infty^+\rangle$ , which exhibits saturated antiferromagnetic long-ranged order; (ii) We consider unitary time evolution with Hamiltonian  $H_\Delta$ . The state of the system at time  $t$  is thus  $|\Phi_t\rangle = \exp(-iH_\Delta t)|\Phi_0\rangle$ . This quench is integrable [30–32] and exact results on the stationary state are available [28, 33–37]. We employ the infinite Time-Evolving Block-Decimation (iTEBD) algorithm [38, 39] to obtain a very accurate description of  $|\Phi_t\rangle$  in the thermodynamic limit. However, the growth of the bipartite entanglement entropy limits the time window accessible by this method. Retaining up to  $\chi_{max} = 1024$  auxiliary states, we are able to reach a time  $t_{max} \simeq 12$  without significant error ( $\lesssim 10^{-3}$ ).

*PDF dynamics.* — Detailed information on how the antiferromagnetic order melts as the system evolves in time is provided by the PDF of the staggered magnetisation  $M_\ell \equiv \sum_{j=1}^{\ell} (-1)^j S_j^z$  of a subsystem of  $\ell$  neighbouring sites

$$P_\ell(m, t) \equiv \langle \Phi_t | \delta(M_\ell - m) | \Phi(t) \rangle, \\ = \sum_{r \in \mathbb{Z}} \tilde{P}_\ell(m, t) \delta(m - r - (1 - (-1)^\ell)/4), \quad (3)$$

where second line follows from the fact that the eigenvalues of  $M_\ell$  are half-integer numbers. We note that the probabilities satisfy the normalisation condition  $\sum_{m=-\ell/2}^{\ell/2} \tilde{P}_\ell(m, t) = 1$ . The initial Néel state is an eigenstate of the staggered subsystem magnetization  $M_\ell$  and concomitantly the probability distribution is a delta func-

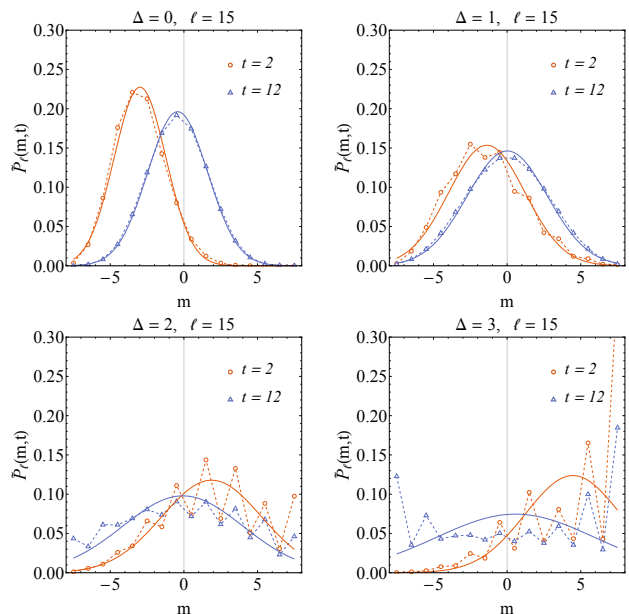


FIG. 2. Snapshots of the rescaled PDF in Fig. 1 at fixed times  $t = 2, 12$ . The numerical data (symbols/dashed lines) are compared to the Gaussian approximation (4) (full lines).

tion  $P_\ell(m, 0) = \delta(m - \ell/2)$ . This reflects the long-range magnetic order in the initial state. In Fig. 1 we show the evolution of  $P_\ell(m, t)$  in time obtained by iTEBD for subsystem size  $\ell = 15$  and several values of the interaction strength  $\Delta$  in the “post-quench” Hamiltonian (2). We observe that the probability distribution depends strongly on  $\Delta$ : for small values of  $\Delta$  the antiferromagnetic short-ranged order melts quickly and  $P_\ell(m, t)$  is narrowly peaked around its average, which exhibits a damped oscillatory behaviour around zero [40]. The behaviour for  $\Delta \gtrsim 2$  is very different: short-ranged order persists for some time while the probability distribution broadens and becomes more symmetric in  $m$ . This nicely chimes with the expectation (see below) that in the stationary state reached at late times the probability distribution to become symmetric in  $m$ . In Fig. 2 we plot the weights of  $P_\ell(m, t)$  at several times and compare them to a Gaussian approximation based on the first two moments  $\bar{m}(t) = \langle \Phi_t | M_\ell | \Psi_t \rangle$ ,  $\sigma^2(t) = \langle \Phi_t | M_\ell^2 | \Psi_t \rangle - \bar{m}^2(t)$

$$P_\ell(\mu, t) = \frac{1}{\sqrt{2\pi\sigma^2(t)}} \exp\left\{-\frac{[\mu - \bar{m}(t)]^2}{2\sigma^2(t)}\right\}. \quad (4)$$

We see that at  $\Delta = 0$  the probability distribution is approximately Gaussian at all times, while for  $\Delta = 2, 3$  it exhibits a pronounced even/odd structure at short times and even at the latest times shown is strongly non-Gaussian. As we are dealing with a one dimensional system at a finite energy density relative to the ground state, we expect  $|\Phi_t\rangle$  to exhibit a time-dependent but finite correlation length. This is borne out by a com-

putation of  $\langle \Phi_t | S_j^z S_{j+n}^z | \Phi_t \rangle$ , which exhibits exponential decay in the distance  $n$ . At time  $t = 6$  the correlation lengths  $\xi(t, \Delta)$  for the values shown in Fig. 1 are  $\xi(6, 0) = 0.424091$ ,  $\xi(6, 1) = 0.925666$ ,  $\xi(6, 2) = 3.39616$  and  $\xi(6, 3) = 8.85259$  respectively. The qualitative dependence of  $\xi(t, \Delta)$  on  $\Delta$  is expected as the energy density imposed by the quench increases with decreasing  $\Delta$ .

*“Small”-  $\Delta$  regime.* — At small values of  $\Delta$  and short and intermediate times we can use a time-dependent self-consistent mean-field approximation to determine the evolution of  $P_\ell(m, t)$ . We first map the Hamiltonian (2) to a model of spinless fermions by means of a Jordan-Wigner transformation, where we use the positive (negative) z-direction in spin space as quantization axis for even (odd) sites [56]. This results in a spinless fermion Hamiltonian

$$H_\Delta = \sum_j \frac{1}{2} [c_j^\dagger c_{j+1}^\dagger + \text{h.c.}] + \Delta n_j (1 - n_{j+1}), \quad (5)$$

where  $n_j = c_j^\dagger c_j$  and  $\{c_j, c_k^\dagger\} = \delta_{j,k}$ . The staggered subsystem magnetization maps to  $M_\ell = \sum_{j=1}^{\ell} (1/2 - n_j)$ , while the initial Néel state maps to the fermion vacuum  $|\Psi_0\rangle = |0\rangle$ . Our self-consistent approximation corresponds to the replacement

$$n_j n_{j+1} \rightarrow \left[ \langle c_j^\dagger c_{j+1}^\dagger \rangle_t c_{j+1} c_j - \langle c_{j+1}^\dagger c_j \rangle_t c_j^\dagger c_{j+1} + \text{h.c.} \right] + \langle n_j \rangle_t n_{j+1} + \langle n_{j+1} \rangle_t n_j, \quad (6)$$

which leads to an explicitly time-dependent Hamiltonian  $H_{\text{MF}}(t)$ , cf. Ref. 42. The expectation values in (6) are calculated self-consistently  $\langle \cdot \rangle_t = \langle \Psi_t | \cdot | \Psi_t \rangle$ , where

$$|\Psi_t\rangle = T \exp \left[ -i \int_0^t dt' H_{\text{MF}}(t') \right] |0\rangle. \quad (7)$$

Following Ref. 44 we can express the characteristic function of  $P_\ell(m, t)$  as a determinant of a  $2\ell \times 2\ell$  matrix [56], which is easily evaluated numerically. This provides us with exact results at  $\Delta = 0$  for all times [56], and a highly accurate short-time approximation even for  $\Delta = 3$  as is shown in Fig. 3.

*Late times.* — We now turn to the behaviour at late times after the quench. The stationary state is characterized by a finite correlation length  $\xi(\Delta)$ . On length scales  $\ell \lesssim \xi(\Delta)$  we expect short-ranged antiferromagnetic order to remain, while it will have melted at scales  $\ell > \xi(\Delta)$ . We also expect the spin-rotational symmetry by  $\pi$  around the x-axis to be restored in the stationary state as we are dealing with a one dimensional system with short-range interactions. The situation is completely analogous to that at finite temperatures – in fact adding a very small integrability-breaking term to the Hamiltonian would result in a steady state that is very close to the thermal state of the XXZ chain [34]. In contrast to the steady state after our quench, the probability distribution of the

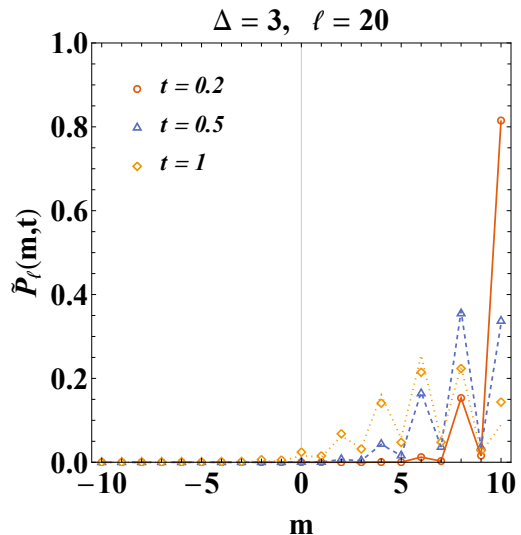


FIG. 3.  $\tilde{P}_\ell(m, t)$  for  $\ell = 20$  at times  $t = 0.2, 0.5, 1$  after a quench from the classical Néel state to a Heisenberg chain with  $\Delta = 3$ . Lines are obtained by the self-consistent fermionic mean-field approximation and the symbols are iTEBD results.

staggered subsystem magnetization at finite temperature  $P_\ell(m, \beta)$  can be computed by matrix product state methods and for the aforementioned reasons it is instructive to consider it. Results for two values of  $\Delta$  are shown in Fig. 4. We see that the probability distributions are symmetric in  $m$ , reflecting the unbroken symmetry of rotations by  $\pi$  around the x-axis. At  $\Delta = 4$  we further observe that when the subsystem size exceeds the thermal correlation length  $\xi_\Delta(\beta)$  antiferromagnetic short-ranged order melts and we obtain a Gaussian probability distribution centred around  $m = 0$ . On the other hand, for  $\ell \lesssim \xi_\Delta(\beta)$  the probability distribution is very broad and peaked at the maximal values  $\pm \ell/2$ , signalling the presence of both kinds of antiferromagnetic short-ranged order. For  $\Delta = 1$  the thermal correlation length is smaller than one lattice site in the temperature regime shown, which is why no traces of short-range order are visible and the probability distribution is a Gaussian centred around  $m = 0$ . The large- $\Delta$  regime is characterized by a low density of excitations and it is therefore possible to understand the behaviour observed above by combining a  $1/\Delta$ -expansion with a linked-cluster expansion [45–53]. As the physics we wish to describe is not tied to integrability, and the non-integrable case is easier to discuss, we focus on the latter [54]. We consider the regime  $\Delta \gg 1$  and break integrability by adding a small perturbation to the Heisenberg Hamiltonian, e.g. consider time evolution under  $H = H_\Delta + \Delta^{-n} V$ , where  $n$  is a positive integer and  $V$  some perturbation involving short-ranged spin-spin interactions that has the same symmetries as  $H_\Delta$ . We define linked clusters following the general for-

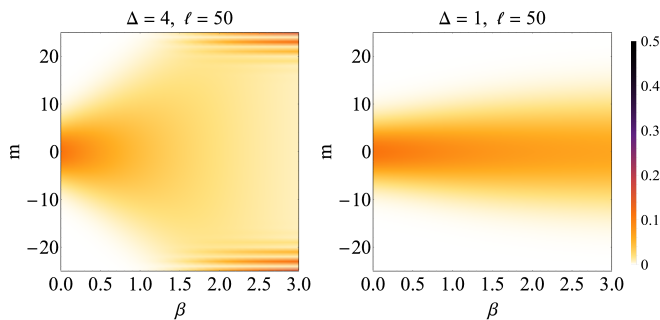


FIG. 4. Density plot of the PDF for the XXZ chain at finite temperature  $1/\beta$  for subsystem size  $\ell = 50$  and  $\Delta = 4$  (left panel);  $\Delta = 1$  (right panel).

malism of Ref. 45 and then implement a  $1/\Delta$ -expansion through a unitary transformation  $\tilde{H} = e^{iS} H e^{-iS}$  [55, 56]. The result is an expansion of the stationary state density matrix of the form

$$\rho_{\text{SS}} = \sum_{j \geq 0} \rho_{\text{SS}}^{(j)}, \quad \rho_{\text{SS}}^{(j)} = \mathcal{O}(e^{-\beta_{\text{eff}} j \Delta/2}), \quad (8)$$

where  $\rho_{\text{SS}}^{(j)}$  are given as power series in  $1/\Delta$ . The leading term in the expansion is  $\rho_{\text{SS}}^{(0)} = \frac{1}{2} \sum_{\sigma=\pm} |\text{GS}_{\Delta}^{\sigma}\rangle \langle \text{GS}_{\Delta}^{\sigma}|$ , where  $|\text{GS}_{\Delta}^{\sigma}\rangle$  are the two ground states of the model at anisotropy  $\Delta$ . The small parameter  $e^{-\beta_{\text{eff}} \Delta/2}$  is proportional to the density of domain-wall excitations over the ground states at large  $\Delta$ . The expansion (8) of the steady-state density matrix leads to a corresponding expansion of the probability distribution of the staggered subsystem magnetization  $P_{\ell}(m, \infty) = \sum_j P_{\ell}^{(j)}(m)$  [56]

$$P_{2\ell}^{(0)}(m) = \delta(\ell - |m|) \left[ \frac{1}{2} - \frac{2\ell + 1}{8\Delta^2} \right] + \delta(\ell - 1 - |m|) \frac{1}{4\Delta^2} + \delta(\ell - 2 - |m|) \frac{2\ell - 1}{8\Delta^2} + o(\Delta^{-2}), \quad (9)$$

$$P_{2\ell}^{(1)}(m) = e^{-\frac{\beta_{\text{eff}} \Delta}{2}} I_0(\beta_{\text{eff}}) \left[ \frac{1 - \ell}{2} \delta(\ell - |m|) + \sum_{j=1}^{\ell} \delta(\ell - j - |m|) \right] + \dots, \quad (10)$$

where the dots denote subleading terms in  $1/\Delta$ . The expansions (10) hold as long as the subsystem size  $2\ell$  is small compared to the correlation length in  $\rho_{\text{SS}}$  and establish that for large anisotropies  $\Delta$  the probability distribution in the steady state is symmetric in  $m$  and close to the average over the two ground states. In addition there is an exponentially suppressed “background” contribution arising from a dilute gas of domain walls.

“Symmetrization” of the PDF in time. — A characteristic feature of the time-evolution of  $P_{\ell}(m, t)$  is that it becomes increasingly symmetric in  $m$ . In order to ascertain the associated time scale in the most interesting

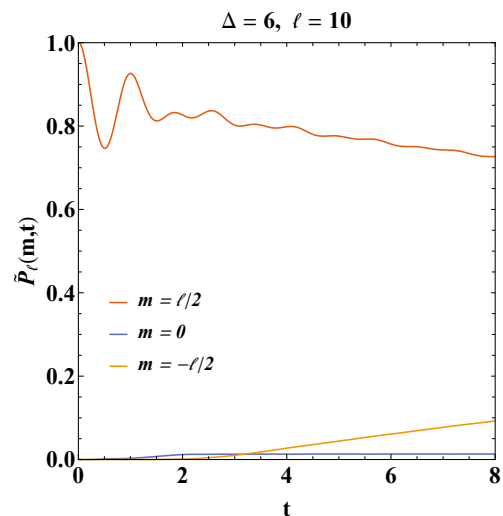


FIG. 5. Weights  $\tilde{P}_{\ell}(m, t)$  for  $\ell = 10$  and a quench from the classical Néel state to a Heisenberg chain with  $\Delta = 6$ . We observe a linear growth (decrease) in time of the weights for  $m = -\ell/2$  ( $m = \ell/2$ ), indicating that the symmetrization of the PDF is driven by ballistic propagation of quasi-particles.

large- $\Delta$  regime it is useful to compare the probabilities for  $M_{\ell}$  to be maximal ( $\ell/2$ ) or minimal ( $-\ell/2$ ) respectively. Results for  $\Delta = 6$  are shown in Fig. 5. We see that  $P_{\ell}(-\ell/2, t)$  grows linearly in time, while  $P_{\ell}(\ell/2, t)$  shows a corresponding linear decrease. For the integrable XXZ chain the associated velocity is expected to be the maximal group velocity of elementary excitations over the stationary state [57]. In presence of weak integrability-breaking interactions in the large- $\Delta$  regime we expect qualitatively similar prethermal behaviour [58].

*Conclusions.* — We have considered the full quantum mechanical order parameter probability distribution  $P_{\ell}(m, t)$  in a subsystem of size  $\ell$  after a quantum quench from a classical Néel state to the spin-1/2 Heisenberg XXZ chain. We have shown that  $P_{\ell}(m, t)$  provides detailed information how short-range antiferromagnetic order melts and have shown how to understand our numerical findings by analytical approaches valid in certain limits. Our setup should be realizable in cold-atom experiments like the ones by the Harvard group [18]. Our findings can be understood in terms of a simple physical picture based on (i) the initial presence of long-ranged order, (ii) the principle of local relaxation after quantum quenches and (iii) the presence of two length scales, namely a finite, time-dependent correlation length  $\xi(t)$  and the sub-system size  $\ell$  in our problem. Initially order is present on all length scales. At sufficiently late times short-ranged order remains on scales  $\ell < \xi(t)$  and is clearly visible in  $P_{\ell}(m, t)$  even though the latter reflects the eventual restoration of the initially broken symmetry. On the other hand the order has melted for larger scales

$\ell > \xi(t)$  and  $P_\ell(m, t)$  is essentially Gaussian. We expect that this physical picture applies quite generally to the melting of long-range order and in particular is not restricted to one dimensional systems as long as the time evolving density matrix is characterized by a finite, time-dependent correlation length. This is generically the case in  $D=1$ , but equally applies to higher dimensional systems at energy densities that correspond to temperatures above any phase transitions. It would be interesting to study the case of quenches that correspond to energy densities corresponding to temperatures below a phase transition.

*Acknowledgments.* — We are grateful to P. Calabrese, A. De Luca and M. Fagotti for stimulating discussions and to the Erwin Schrödinger International Institute for Mathematics and Physics for hospitality and support during the programme on *Quantum Paths*. M.C. thanks the Galileo Galilei Institute in Florence for hospitality during the workshop “Entanglement in quantum systems”. This work was supported by the the European Union’s Horizon 2020 under the Marie Skłodowska-Curie grant agreement No. 701221 NET4IQ (M.C. and F.H.L.E.), the EPSRC under grant EP/N01930X (F.H.L.E.), the National Science Foundation under Grant No. NSF PHY-1748958 (F.H.L.E.), by the BMBF and EU-Quantera via QTFLAG (M.C.), and the Quantum Flagship via PASQuaS (M. C.).

- 
- [1] T. Langen, R. Geiger and J. Schmiedmayer, *Ultracold Atoms Out of Equilibrium*, *Ann. Rev. Cond. Matt. Phys.* **6**, 201 (2015).
- [2] E. Altman, *Nonequilibrium quantum dynamics in ultracold quantum gases in Strongly Interacting Quantum Systems out of Equilibrium: Lecture Notes of the Les Houches Summer School*, eds T. Giamarchi, A.J. Millis, O. Parcollet, H. Saleur and L.F. Cugliandolo, **99** (2012).
- [3] T. Kinoshita, T. Wenger, D. S. Weiss, *A quantum Newton’s cradle*, *Nature* **440**, 900 (2006).
- [4] M. Greiner, O. Mandel, T.W. Hänsch, and I. Bloch, *Collapse and revival of the matter wave field of a Bose-Einstein condensate*, *Nature* **419**, 51-54 (2002).
- [5] L. Hackermüller, U. Schneider, M. Moreno-Cardoner, T. Kitagawa, S. Will, T. Best, E. Demler, E. Altman, I. Bloch and B. Paredes, *Anomalous Expansion of Attractively Interacting Fermionic Atoms in an Optical Lattice*, *Science* **327**, 1621 (2010).
- [6] S. Trotzky Y.-A. Chen, A. Flesch, I. P. McCulloch, U. Schollwöck, J. Eisert, and I. Bloch, *Probing the relaxation towards equilibrium in an isolated strongly correlated 1D Bose gas*, *Nature Phys.* **8**, 325 (2012).
- [7] U. Schneider, L. Hackermüller, J. P. Ronzheimer, S. Will, S. Braun, T. Best, I. Bloch, E. Demler, S. Mandt, D. Rasch, and A. Rosch, *Fermionic transport and out-of-equilibrium dynamics in a homogeneous Hubbard model with ultracold atoms*, *Nature Phys.* **8**, 213 (2012).
- [8] M. Cheneau, P. Barmettler, D. Poletti, M. Endres, P. Schauss, T. Fukuhara, C. Gross, I. Bloch, C. Kollath, and S. Kuhr, *Light-cone-like spreading of correlations in a quantum many-body system*, *Nature* **481**, 484 (2012).
- [9] T. Langen, R. Geiger, M. Kuhnert, B. Rauer, and J. Schmiedmayer, *Local emergence of thermal correlations in an isolated quantum many-body system*, *Nature Phys.* **9**, 640 (2013).
- [10] F. Meinert, M.J. Mark, E. Kirilov, K. Lauber, P. Weinmann, A.J. Daley, and H.-C. Nägerl, *Quantum Quench in an Atomic One-Dimensional Ising Chain*, *Phys. Rev. Lett.* **111**, 053003 (2013).
- [11] J.P. Ronzheimer, M. Schreiber, S. Braun, S.S. Hodgman, S. Langer, I.P. McCulloch, F. Heidrich-Meisner, I. Bloch and U. Schneider, *Expansion dynamics of interacting bosons in homogeneous lattices in one and two dimensions*, *Phys. Rev. Lett.* **110**, 205301 (2013).
- [12] N. Navon, A.L. Gaunt, R.P. Smith and Z. Hadzibabic, *Critical Dynamics of Spontaneous Symmetry Breaking in a Homogeneous Bose gas*, *Science* **347**, 167 (2015).
- [13] Y. Tang, W. Kao, K.-Y. Li, S. Seo, K. Mallayya, M. Rigol, S. Gopalakrishnan and B.L. Lev, *Thermalization near integrability in dipolar quantum Newton’s cradle*, *Phys. Rev. X* **8**, 021030 (2018).
- [14] S. Hofferberth, I. Lesanovsky, T. Schumm, A. Imambekov, V. Gritsev, E. Demler, and J. Schmiedmayer, *Probing quantum and thermal noise in an interacting many-body system*, *Nature Phys.* **4**, 489 (2008).
- [15] T. Kitagawa, S. Pielawa, A. Imambekov, J. Schmiedmayer, V. Gritsev, and E. Demler, *Ramsey Interference in One-Dimensional Systems: The Full Distribution Function of Fringe Contrast as a Probe of Many-Body Dynamics*, *Phys. Rev. Lett.* **104**, 255302 (2010).
- [16] T. Kitagawa, A. Imambekov, J. Schmiedmayer, and E. Demler, *The dynamics and prethermalization of one-dimensional quantum systems probed through the full distributions of quantum noise*, *New J. Phys.* **13**, 73018 (2011).
- [17] M. Gring, M. Kuhnert, T. Langen, T. Kitagawa, B. Rauer, M. Schreitl, I. Mazets, D. A. Smith, E. Demler, and J. Schmiedmayer, *Relaxation and Prethermalization in an Isolated Quantum System*, *Science* **337**, 1318 (2012).
- [18] A. Mazurenko, C.S. Chiu, G. Ji, M.F. Parsons, M. Kanasz-Nagy, R. Schmidt, F. Grusdt, E. Demler, D. Greif and M. Greiner, *Experimental realization of a long-range antiferromagnet in the Hubbard model with ultracold atoms*, *Nature* **545**, 462 (2017).
- [19] M. Först et al, *Melting of Charge Stripes in Vibrationally Driven  $\text{La}_{1.875}\text{Ba}_{0.125}\text{CuO}_4$  : Assessing the Respective Roles of Electronic and Lattice Order in Frustrated Superconductors*, *Phys. Rev. Lett.* **112**, 157002 (2014).
- [20] R. Mankowsky, M. Först and A. Cavalleri, *Non-equilibrium control of complex solids by nonlinear phononics*, *Rep. Progr. Phys.* **79** 064503 (2016).
- [21] H. Seo, Y. Tanaka and S. Ishihara, *Photoinduced collective mode, inhomogeneity, and melting in a charge-order system*, *Phys. Rev. B* **98**, 235150 (1028).
- [22] J. M. Deutsch, *Quantum statistical mechanics in a closed system*, *Phys. Rev. A* **43**, 2046 (1991).
- [23] M. Srednicki, *Chaos and quantum thermalization*, *Phys. Rev. E* **50**, 888 (1994).
- [24] M. Rigol, V. Dunjko, and M. Olshanii, *Thermalization and its mechanism for generic isolated quantum systems*, *Nature* **452**, 854 (2008).

- [25] M. Rigol, V. Dunjko, V. Yurovsky, and M. Olshanii, *Relaxation in a Completely Integrable Many-Body Quantum System: An Ab Initio Study of the Dynamics of the Highly Excited States of 1D Lattice Hard-Core Bosons*, *Phys. Rev. Lett.* **98**, 50405 (2007).
- [26] A. C. Cassidy, C. W. Clark, and M. Rigol, *Generalized Thermalization in an Integrable Lattice System*, *Phys. Rev. Lett.* **106**, 140405 (2011).
- [27] J.-S. Caux and F.H.L. Essler, *Time Evolution of Local Observables After Quenching to an Integrable Model*, *Phys. Rev. Lett.* **110**, 257203 (2013).
- [28] E. Ilievski, J. De Nardis, B. Wouters, J.-S. Caux, F.H.L. Essler, T. Prosen, *Complete Generalized Gibbs Ensemble in an interacting Theory*, *Phys. Rev. Lett.* **115**, 157201 (2015).
- [29] In the sense that nearby spins are strongly antiferromagnetically correlated.
- [30] B. Pozsgay, *The generalized Gibbs ensemble for Heisenberg spin chains*, *J. Stat. Mech.* P07003 (2013).
- [31] M. Fagotti and F.H.L. Essler, *Stationary behaviour of observables after a quantum quench in the spin-1/2 Heisenberg XXZ chain*, *J. Stat. Mech.* P07012 (2013).
- [32] M. Fagotti, M. Collura, F.H.L. Essler, and P. Calabrese, *Relaxation after quantum quenches in the spin-1/2 Heisenberg XXZ chain*, *Phys. Rev. B* **89**, 125101 (2014).
- [33] B. Wouters, J. De Nardis, M. Brockmann, D. Fioretto, M. Rigol, J.-S. Caux, *Quenching the Anisotropic Heisenberg Chain: Exact Solution and Generalized Gibbs Ensemble Predictions*, *Phys. Rev. Lett.* **113**, 117202 (2014).
- [34] M. Brockmann, B. Wouters, D. Fioretto, J. De Nardis, R. Vlijm and J.-S. Caux, *Quench action approach for releasing the Néel state into the spin-1/2 XXZ chain*, *Stat. Mech.* P12009 (2014).
- [35] B. Pozsgay, M. Mestyán, M.A. Werner, M. Kormos, G. Zaránd, and G. Takács, *Correlations after Quantum Quenches in the XXZ Spin Chain: Failure of the Generalized Gibbs Ensemble*, *Phys. Rev. Lett.* **113**, 117203 (2014).
- [36] M. Mestyán, B. Pozsgay, G. Takács, and M.A. Werner, *Quenching the XXZ spin chain: quench action approach versus generalized Gibbs ensemble*, *J. Stat. Mech.* P04001 (2015).
- [37] E. Ilievski, E. Quinn, J. De Nardis and M. Brockmann, *String-charge duality in integrable lattice models*, *J. Stat. Mech.* 063101 (2016).
- [38] G. Vidal, *Classical Simulation of Infinite-Size Quantum Lattice Systems in One Spatial Dimension*, *Phys. Rev. Lett.* **98**, 070201 (2007).
- [39] R. Orús and G. Vidal, *Infinite time-evolving block decimation algorithm beyond unitary evolution*, *Phys. Rev. B* **78**, 155117 (2008).
- [40] P. Barmettler, M. Punk, V. Gritsev, E. Demler, and E. Altman, *Relaxation of antiferromagnetic order in spin-1/2 chains following a quantum quench*, *Phys. Rev. Lett.* **102**, 130603 (2009).
- [41] P. Barmettler, M. Punk, V. Gritsev, E. Demler, and E. Altman, *Quantum quenches in the anisotropic spin-1/2 Heisenberg chain: different approaches to many-body dynamics far from equilibrium*, *New J. Phys.* **12**, 055017 (2010).
- [42] S. Sotiriadis and J. Cardy, *Quantum quench in interacting field theory: A self-consistent approximation*, *Phys. Rev. B* **81**, 134305 (2010).
- [43] Y.D. van Nieuwerkerk and F.H.L. Essler, *Self-consistent time-dependent harmonic approximation for the Sine-Gordon model out of equilibrium*, [arXiv:1812.06690](https://arxiv.org/abs/1812.06690).
- [44] S. Groha, F.H.L. Essler and P. Calabrese, *Full Counting Statistics in the Transverse Field Ising Chain*, *SciPost Phys.* **4**, 043 (2018).
- [45] F.H.L. Essler and R.M. Konik, *Finite Temperature Dynamical Correlations in Massive Integrable Quantum Field Theories*, *J. Stat. Mech.* P09018 (2009).
- [46] A.J.A. James, F.H.L. Essler and R.M. Konik, *Finite Temperature Dynamical Structure Factor of Alternating Heisenberg Chains*, *Phys. Rev. B* **78**, 094411 (2008).
- [47] W.D. Goetze, U. Karahasanovic and F.H.L. Essler, *Low-Temperature Dynamical Structure Factor of the Two-Leg Spin-1/2 Heisenberg Ladder*, *Phys. Rev. B* **82**, 104417 (2010).
- [48] B. Pozsgay and G. Takacs, *Form factor expansion for thermal correlators*, *J. Stat. Mech.* P11012 (2010).
- [49] I.M. Szecsenyi and G. Takacs, *Spectral expansion for finite temperature two-point functions and clustering*, *J. Stat. Mech.* P12002 (2012).
- [50] P. Calabrese, F.H.L. Essler, and M. Fagotti, *Quantum Quench in the Transverse-Field Ising Chain*, *Phys. Rev. Lett.* **106**, 227203 (2011).
- [51] P. Calabrese, F.H.L. Essler, and M. Fagotti, *Quantum quench in the transverse field Ising chain: I. Time evolution of order parameter correlators*. *J. Stat. Mech.* P07016 (2012).
- [52] D. Schuricht and F.H.L. Essler, *Dynamics in the Ising field theory after a quantum quench*, *J. Stat. Mech.*, P04017 (2012).
- [53] B. Bertini, D. Schuricht, and F.H.L. Essler, *Quantum quench in the sine-Gordon model*, *J. Stat. Mech.* P10035 (2014).
- [54] We stress that the differences between the integrable and non-integrable cases occur only at higher orders in the expansion and our results therefore apply to both cases.
- [55] A. H. MacDonald, S. M. Girvin, D. Yoshioka, *Phys. Rev. B* **37**, 16 (1988).
- [56] See Supplemental Material at [URL will be inserted by publisher] for further details about self-consistent time dependent mean-field approximation, as well as the large- $\Delta$  expansion for the stationary probability distribution function of the order parameter.
- [57] L. Bonnes, F.H.L. Essler and A. Läuchli, *“Light-Cone” Dynamics After Quantum Quenches in Spin Chains*, *Phys. Rev. Lett.* **113**, 187203 (2014).
- [58] B. Bertini, F.H.L. Essler, S. Groha, N.J. Robinson, *Thermalization and light cones in a model with weak integrability breaking*, *Phys. Rev. B* **94**, 245117 (2016).
- [59] M. Fagotti and P. Calabrese, *Entanglement entropy of two disjoint blocks in XY chains*, *J. Stat. Mech.* P04016 (2010).